

NEW ASPECTS OF BEAM-BEAM PHENOMENA IN HADRON COLLIDERS

T. Sen *, FNAL, Batavia, IL 60510, USA

Abstract

Long-range beam-beam interactions in Run II at the Tevatron are the dominant sources of beam loss and lifetime limitations of anti-protons, especially at injection energy. The main focus of the talk will be observations of the long-range effects during Run II and theoretical understanding of these effects.

INTRODUCTION

The Tevatron is currently delivering luminosities close to $4 \times 10^{31} \text{ cm}^{-2} \text{ sec}^{-1}$ to the CDF and D0 experiments. In a record store on May 2nd, 2003, (average initial luminosity = $4.2 \times 10^{31} \text{ cm}^{-2} \text{ sec}^{-1}$), the average bunch intensities at the start of collisions were $N_p = 1.96 \times 10^{11}$, $N_{\bar{p}} = 0.25 \times 10^{11}$. These are to be compared with design values for Run II of 2.7×10^{11} and 1.35×10^{11} for protons and anti-protons respectively. Beam-beam effects have generally been more severe on the anti-protons but with increasing anti-proton intensity, their effects on protons are also increasing. I will review the beam-beam effects at various stages of the operational cycle of the Tevatron.

After 36 bunches of protons are injected and placed on the proton helix, anti-protons are injected four bunches at a time. After all bunches are injected, acceleration to top energy takes about 85 seconds. After reaching flat top, the optics around the interaction regions (IRs) is changed to lower β^* from 1.6 m to 0.35 m at B0 and D0 and the beams are brought into collision. During a high energy physics store each bunch experiences two head-on collisions with bunches in the opposing beam and seventy long-range interactions. At all other stages, each bunch experiences only long-range interactions - seventy two in all.

THEORETICAL ANALYSIS OF BEAM-BEAM INTERACTIONS

Beam-beam forces change the linear and nonlinear dynamics of particles in fundamental ways. The long-range beam-beam force has in general both quadrupolar and skew-quadrupolar components. The magnitude of the tune and coupling shift depends on the beam separation but also on the amplitude of the particle experiencing the force. Since there is dispersion at the locations of the long-range interactions in the Tevatron, the separation between the test particle and the other beam and therefore the tune shift depends on the momentum deviation of the particle. An amplitude dependent tune shift implies that the chromaticity

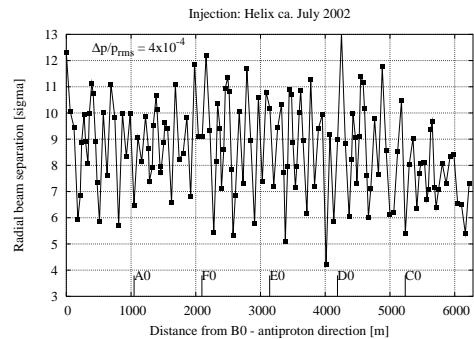


Figure 1: Beam separations at all the parasitics at 150 GeV with the design value for the proton momentum spread and the present injection helix.

shift is also amplitude dependent. These amplitude dependences introduce the familiar tune footprint but also coupling and chromaticity footprints within a bunch.

Theoretical expressions have been developed for the amplitude dependent tune shifts, chromaticities and coupling for arbitrary aspect ratios [1] because the proton beam is not round at most of the long-range interactions. Some conclusions are easily drawn however from the round beam case. At large distances, both the tune shift and the coupling fall as $1/d^2$ while the chromaticity falls off more rapidly as $1/d^3$. The tune shift for round beams vanishes if the plane of the helix is at 45° . Minimizing the chromaticity requires the plane of the helix to be either at 30° or vertical. The coupling vanishes if the separation is either in the horizontal or the vertical plane. Since each of these parameters has a different dependence on the helix angle, it is not possible to minimize them simultaneously with a choice of the angle.

Each anti-proton bunch sees a different sequence of long-range interactions with different optics functions. This leads to a significant spread of tune shifts, coupling and chromaticities between the bunches. Thus the working point for example cannot be optimized for all bunches at once. Due to the amplitude dependence of these quantities, the spread within a bunch can be comparable to the spread between the bunches.

Injection Energy

There are 138 different locations of parasitic interactions around the ring. Figure 1 shows the beam separations with the present helix and assuming the design value of $(\Delta p/p)_{rms}$. The smallest separation is about 4σ close to D0 but there is a large variation between $5-12\sigma$ at most of the other parasitics. At most parasitics the beta func-

* tsen@fnal.gov

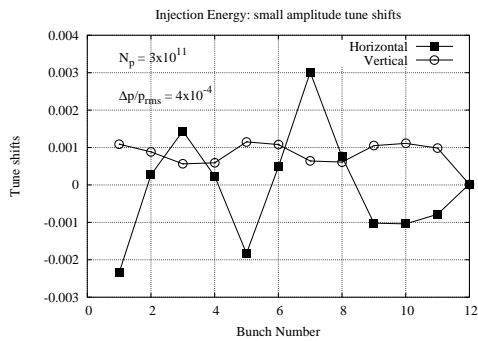


Figure 2: Beam-beam induced tune shifts of anti-protons at small amplitude, bunch by bunch.

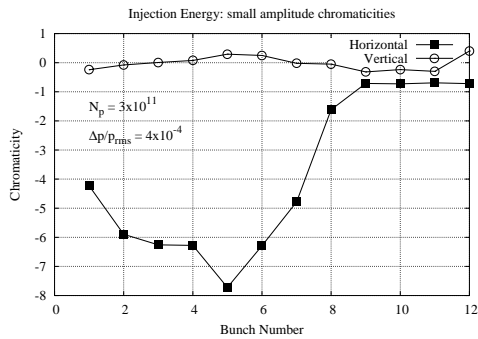


Figure 3: Beam-beam induced chromaticity at small amplitude, bunch by bunch (150 GeV).

tions are larger in the horizontal plane. This asymmetry in the beta functions is reflected in parameters like the tune shifts.

Figure 2 shows the small amplitude tune shifts of the anti-protons, bunch by bunch. The tune footprint at large amplitudes however is determined by the machine nonlinearities which change the sign of the detuning.

The beam-beam induced global coupling at small amplitude is of the same magnitude as the lattice induced global coupling. Figure 3 shows the small amplitude chromaticity. The large spread in chromaticity could make some bunches more sensitive to synchro-betatron resonances and to coherent instabilities at high anti-proton intensities. Bunch 12 suffers the least changes to its tune, coupling and chromaticity from the beam-beam interactions at injection.

Resonance driving terms have been calculated from a nonlinear map, first with only the lattice nonlinearities and second with the lattice and the beam-beam nonlinearities for anti-proton bunch 1. The lattice nonlinearities include the correction sextupoles and the error fields in the magnets. These terms were evaluated along the diagonal at an amplitude of 2σ , and the largest resonance strength was normalized to 1. The resonance condition is $p\nu_x + q\nu_y = \text{integer}$. Fourth order resonances are driven strongly by the lattice, the largest of these being the difference (2,-2) resonance. Addition of the beam-beam effects shows that they dominate the lattice resonances, as seen in Figure 4

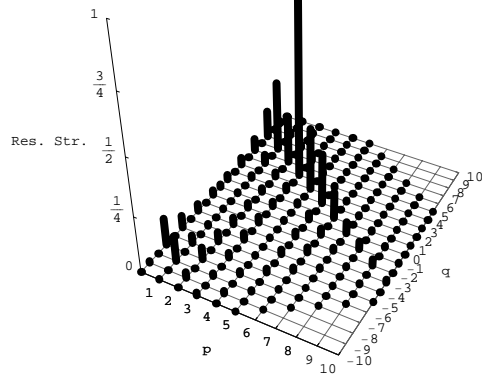


Figure 4: Resonance strengths at injection at an amplitude of 2σ with lattice and beam-beam nonlinearities.

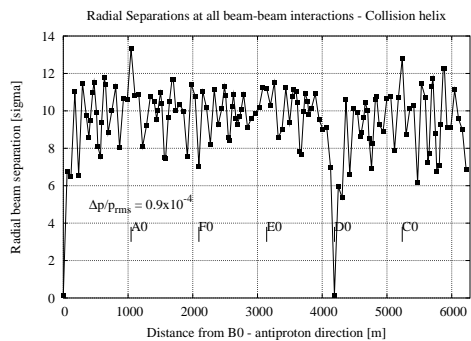


Figure 5: Beam separations at all the parasitics at 980 GeV with expected values for the proton momentum spread.

which has a completely different resonance pattern. The beam-beam fields drive the seventh order resonances, the strongest at this amplitude being the (3, 4) resonance.

The large energy spread at injection makes synchrobetatron resonances also important. Calculations [2] show that at present chromaticities and energy spreads, the synchrotron sidebands of some betatron resonances are wide enough to overlap which may lead to faster diffusion. A smaller energy spread at injection would therefore increase the dynamic aperture at injection.

Collision

The smallest separations at the parasitic collisions occur at the ones immediately upstream and downstream of the head-on collisions at B0 and D0. Figure 5 shows the beam separations around the ring. The beta functions at these four parasitics are also the largest. Consequently the tune shifts and resonance driving terms (for example) contain the largest contributions from these parasitics amongst all the parasitics.

The bunch by bunch variation in tunes is quite different from the variation at injection [cf. Figure 2]. Only the

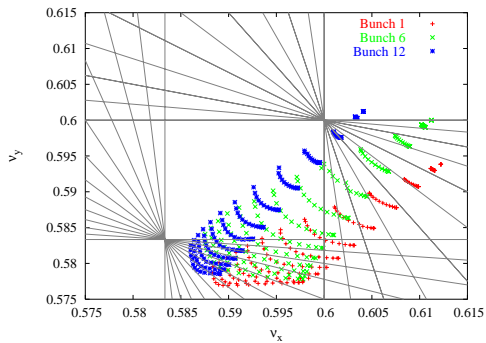


Figure 6: Tune footprints of bunches 1, 6 and 12 superposed on the 5th and 12th order sum resonances.

head (bunch 1) and the tail (bunch 12) of the train have tune shifts significantly different from the others. Bunch 1 does not suffer the first parasitic upstream (where β_y is large) of the IPs and bunch 12 misses the first parasitic downstream (where β_x is large) of the IPs. Figure 6 shows the tune footprint (up to 6σ) of these bunches and that of bunch 6 which is representative of all the other bunches. The extent of the footprint is largely determined by the head-on collisions for all bunches. The beam-beam induced coupling at small amplitudes is smaller than at injection. The beam-beam induced chromaticity (both the variation over the bunches and the magnitude) is larger than at injection.

The head-on collisions create the strongest nonlinear fields but drive only even order resonances, mainly the 12th order resonances. The effects of these resonances is considerably weakened (by two orders of magnitude at some amplitudes) as a consequence of phase averaging [1]. However with increasing chromaticity the number of synchrotron sidebands with significant width increases as well which increases the effective width of the resonances. The long-range interactions drive the odd order 5th and 7th order resonances. The relatively large chromaticity generated by these interactions create synchrotron sidebands of these resonances which overlap at relatively small amplitudes.

A nonlinear Taylor map has been used to calculate the resonances with both lattice and beam-beam nonlinearities. As at injection, we find that at an amplitude of $2\sigma_p$, the 7th and 5th order resonances driven by the beam-beam dominate. The largest of these are the (3, 4) and (3, 2) resonances. Compared to injection, there are now many more resonances of comparable strength but the strengths themselves are smaller.

SIMULATIONS AND EXPERIMENTS

Injection

The beam-beam interactions have a strong influence on the anti-proton lifetime at 150 GeV. During a study in September 2002 with only anti-protons injected into the Tevatron, the lifetimes at 150 GeV varied between 10-25 hours compared to lifetimes of 1-10 hours in stores. The

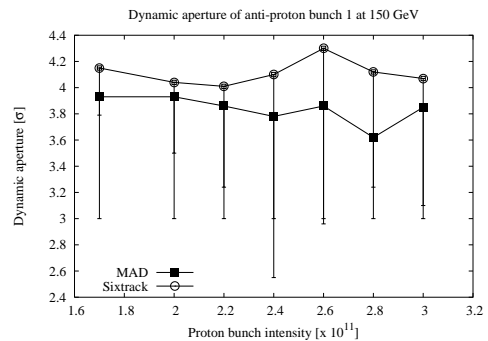


Figure 7: Dynamic aperture after 10^6 turns of anti-proton bunch 1 vs proton intensity at injection. The average value (over all angles in coordinate space) along with one-sided error bars to represent the minimum value at each intensity are shown.

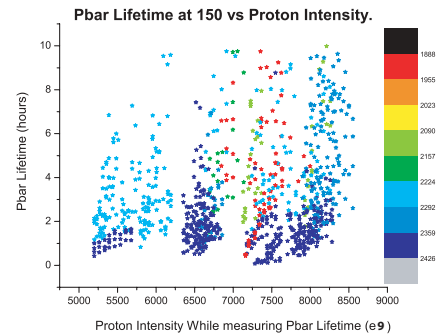


Figure 8: Lifetime of anti-proton bunches vs proton intensities in several recent stores.

losses during acceleration were also small about 2%, compared to typical losses around 10% in stores.

The dynamic aperture of a few anti-proton bunches at 150 GeV has been calculated with extensive simulations. The nonlinearities in the model include the measured multipoles in the magnets, the chromaticity and feed-down sextupoles together with the beam-beam interactions. The results from two different codes, MAD and Sixtrack, typically agree to within 15%. Tracking results show for example that the dynamic aperture with beam-beam interactions drops by about $3\sigma_p$ compared to the case without beam-beam interactions. Figure 7 shows a plot of the average dynamic aperture (after 10^6 turns or 2 seconds in the Tevatron) as a function of the proton bunch intensity. The averaging is done over several initial angles of the particles in physical space. This plot predicts that the dynamic aperture at 150 GeV is about $3\sigma_p$ and nearly independent of the proton intensities over this range.

Figure 8 shows the lifetime of anti-protons at 150 GeV as a function of proton intensity over several recent stores. The lifetimes of most bunches varies between 2-10 hours under typical conditions but is observed to be relatively independent of the proton intensities obtained so far - in

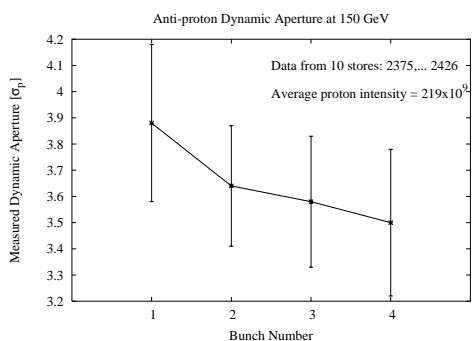


Figure 9: Dynamic aperture of the first four anti-proton bunches at injection calculated from the measured drop in emittance in 10 recent stores. The error bars represent the variation over the stores.

agreement with the result expected from Figure 7. In several recent stores, the emittance of the anti-protons was observed to decrease with time after injection. An example is seen in Figure 10. We consider the first four bunches injected since their emittances are measured 10 times with the flying wires before acceleration. The dynamic aper-

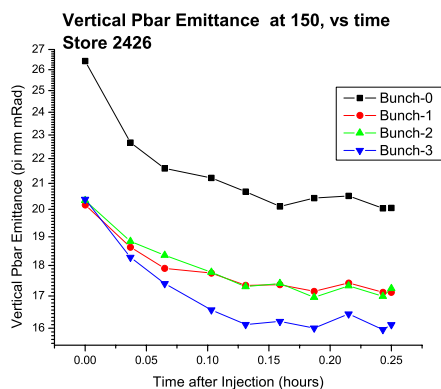


Figure 10: Drop in vertical emittance of the first four anti-proton bunches after injection in a recent store. The asymptotic emittance of each bunch is a measure of its dynamic aperture.

ture was calculated from the asymptotic emittance for 10 recent stores where there was an observed emittance reduction. The dynamic apertures, shown in Figure 9, are in good agreement with the simulation results in Figure 7.

Vertical dampers were recently re-commissioned at injection. The vertical chromaticity can now be dropped from 8 to 4 units while keeping the protons stable. At this lower chromaticity we have not observed the sharp drop in anti-proton emittance during injection. The dynamic aperture has therefore increased from the value shown in Figure 9.

A. Kabel at SLAC has developed a six-dimensional code called PlibB for lifetime simulations. An interesting prediction from one of his simulations is a significant increase

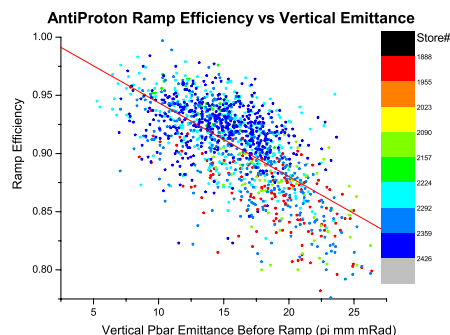


Figure 11: Anti-proton ramp efficiency vs anti-proton vertical emittance in several recent stores.

in the lifetime when the vertical chromaticity is reduced below 4 units. Another parallel code called BeamBeam3D has been developed by J. Qiang at SLAC. As with Kabel's code, the only nonlinearities included so far are those due to the beam-beam interactions. Lifetimes from simulations using this code can be in the range of 1-2 hrs if the physical aperture is small enough. Further development will include the nonlinearities of the magnets.

Ramp and squeeze

A significant fraction of proton losses during the ramp occur in the first 20 seconds while the bucket area is shrinking. Dedicated studies have shown that the proton losses are determined by the longitudinal emittance and the quality of coalescing in the Main Injector. Beam-beam effects on protons during the ramp do not appear to be significant until now. Anti-proton losses during the ramp were measured to be ~2% during a dedicated anti-proton only store in September 2002. However during regular stores with protons present, anti-proton losses averaged around 11% in March 2003. These losses occur during the entire ramp.

The beam separations (in scaled units) are kept constant from 150 GeV to 500 GeV by increasing the separator voltages proportionally to \sqrt{E} . At higher energies there is not enough separator strength to maintain constant separations so the beam separations fall by about 30% during the second half of the ramp. Mitigating the beam-beam driven loss requires an increase in the beam separations during the entire ramp with a different combination of separators.

The anti-proton loss during the ramp is also well correlated with the anti-proton vertical emittance, as seen in Figure 11. Reducing the emittance blow-up while injecting anti-protons in the Tevatron onto the anti-proton helix would therefore also reduce the loss during the ramp. The longitudinal emittance does not appear to have much influence on the anti-proton losses during the ramp.

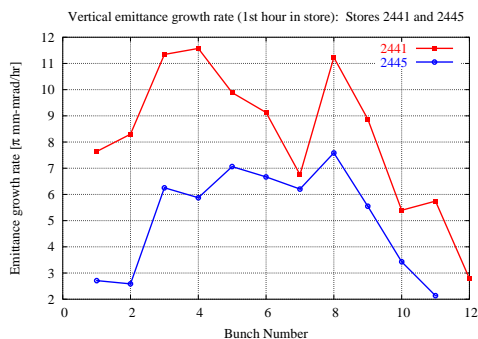


Figure 12: Bunch by bunch vertical emittance growth rates at the beginning of two recent stores. Lowering the vertical tune by 0.001 helped lower the growth rate in Store 2445.

Collision

Extensive dynamic aperture and other tracking calculations at collision optics and Run II design parameters lead to several conclusions. For example, the head-on interactions largely determine the tune footprint but they have very little influence on the dynamic aperture. Of the seventy long-range interactions, the four interactions nearest to the two IPs are the most important in determining the DA but the synchro-betatron resonances driven by the other long-range interactions are important. These calculations also predict that the DA will drop by about 1σ from present intensities ($N_p \sim 210 \times 10^9$) to design intensity ($N_p = 270 \times 10^9$). Analysis of data shows that at present the anti-proton lifetime during stores is not strongly influenced by the beam-beam effects.

In several dedicated studies we have explored the possibility of improving the anti-proton lifetime by changing the collision helix. In the first set of studies (done in August and September of 2002), the helix size in the short arc (between B0 and D0 in the proton direction) was changed. This changed the separation at two of the four parasitics nearest the IPs. Opening the helix vertically seemed to improve the lifetime in the experiment. In subsequent stores the helix was increased vertically by 8% in the short arc but no significant improvement of anti-proton lifetimes was observed. Opening the helix horizontally in the short arc at the start of a few stores did not also show much improvement in the lifetime.

More recently in a study done on March 21, 2003, at the end of a store, the helix was changed in the entire ring and in both planes simultaneously. Losses stayed nearly the same when the helix was opened by 20%. On decreasing the helix size, the losses in both beams decreased at first - perhaps due to the beams moving away from the collimators in the long arc. When the helix was reduced by more than 80%, losses climbed - a combination of beam-beam effects and tunes changing with the helix size. The experimental results from increasing the helix size at collision have therefore been somewhat mixed so far.

Emittance growth at the start of a store has occasionally

been a concern. In most of these cases the anti-proton emittance growth rate was large at the start, then dropped with falling beam intensities. This emittance growth is strongly bunch dependent; typically bunches 1 and 12 have lower growth rates than the others. Small changes to the tune usually suffice to lower the growth rate. Figure 12 shows an example from two recent stores. In Store 2441 the growth rate was large for most bunches. In Store 2445 lowering the vertical tune by 0.001 reduced the growth significantly. Even with the lower growth rate there are differences amongst bunches due to the differences in bunch tunes. More details about experimental beam-beam studies can be found in a companion paper [3].

SUMMARY

We summarize the status of beam-beam effects in the Tevatron. At injection energy they limit the anti-proton lifetime to under 10 hrs but have not influenced proton lifetimes much. During the ramp anti-proton losses (and perhaps emittance growth) are largely due to beam-beam effects. Occasional proton losses, large enough to quench the Tevatron, during the final coggling and squeeze are attributed to beam-beam effects. Proton losses during luminosity are occasionally much higher than observed during machine studies with only protons of similar intensities. Lifetimes of both anti-protons and protons at collision however are largely determined by luminosity with a comparable contribution from residual gas scattering to the proton lifetime.

We are vigorously pursuing several ways of reducing beam-beam limitations at all stages. New helical solutions that increase the separations are being developed and tested using the present set of electrostatic separators. There are also plans to install additional separators around the IPs to increase the separations at the nearest parasitics. Other planned measures include (a) Improving the alignment in the Tevatron, (b) Injecting beams with smaller emittances, (c) Operating with lower chromaticities, (d) Testing different bunch patterns, (e) Improving the IR optics, (f) Searching for better working points, (g) Active compensation of beam-beam effects with the Tevatron electron lens [4] and perhaps in tandem, compensation with current carrying wires.

REFERENCES

- [1] T. Sen, B. Erdelyi, M. Xiao, *Theoretical studies of beam-beam effects in the Tevatron at collision energy*, these proceedings.
- [2] Y. Alexahin, *Beam-beam effects at injection*, http://www-bdnew.fnal.gov/beam-physics-studies/Notes/2002/bb_SBR_at_Linj.pdf
- [3] X.L. Zhang et al., *Experimental studies of beam-beam effects at the Tevatron*, this conference
- [4] K. Bishofberger, this conference